Influence of Coating Thickness on Residual Stress and Bond-Strength of Cold-Sprayed Inconel 718 Coatings

R. Singh[1], S. Schruefer[2], S. Wilson[3], J. Gibmeier[4] and R. Vassen[1]

[1]Institute of Energy and Climate Research (IEK-1), Forschungszentrum-Jülich, 52428-Jülich, Germany
[2]Rolls-Royce Deutschland Ltd & Co KG, Eschenweg 11, Dahlewitz, D-15827 Blankenfelde-Mahlow, Germany
[3]Oerlikon Metco AG, Wohlen, Rigackerstrasse 16, 5610 Wohlen AG, Switzerland
[4]Institute for Applied Materials (IAM-WK), Engelbert-Arnold-Strasse 4, Karlsruhe Institute of Technology, 76131-Karlsruhe, Germany

Abstract

In the cold spray process, deposition of particles takes place through intensive plastic deformation upon impact in a solid state at the temperatures well below their melting point. The high particle impact velocity causes high local stresses which lead to deforming the particles and the substrate plastically in the proximity of the particle–substrate interface. As a result, high residual stresses are introduced in cold spray coating due to the peening effect of the particles collisions with the substrate. In this study, Inconel 718 powder particles were cold-sprayed on Inconel 718 substrates by using nitrogen gas for an application as a repair tool for aero engine components. The magnitude of the residual stress and its distribution through the thickness were measured by using the hole-drilling and the bending methods. Residual stress was also estimated by using Tsui and Clyne's progressive deposition model and by using an approach based on physical process parameters. Mainly compressive residual stresses were observed in cold-sprayed Inconel 718 coatings. Accumulation of residual stresses in the coatings is highly affected by peening during deposition and it decreases with increase in thickness. It has been observed that the bond-strengths of cold-sprayed Inconel 718 coatings are highly influenced by coating thickness and residual stress states of the coating/substrate system. In the presence of residual stresses in the coatings, bond-strength decreases with increasing coating thickness. The energy-release-rate criterion has been used to predict bond-strength with increasing coating thickness. Predicted bond-strength values are close to the measured bond-strength values and decrease with increase in coating thickness.

Keywords: *cold spray; residual stresses; adhesion-strength; Inconel 718*

1. Introduction

Cold spray is a solid-state process, where powder particle (5-50 μm) accelerated towards the substrate by supersonic gas jet through a De Laval nozzle. Powder particle exit the nozzle with supersonic velocities (300-1200 m/s) and impact upon the substrate, where it plastically deforms and create the mechanical and metallurgical bond with substrate material [1-5]. In general, cold spray can produce thick coatings with high density, no oxidation, no phase change, and minimal thermal input [6, 7]. In present times, primary applications of cold gas spray technology are the surface enhancement of sprayed metals and metallic alloys to improve properties such as resistance to wear, erosion, and corrosions. Surface enhancements also lead to produce a free standing shape in the solid state. Thus cold spray has enormous potential for applications which involve material buildup such as for repair, refurbishment, and additive manufacturing [8-11]. Such applications need the coating integrity which depends on the adhesion strength between particles and the substrate and among the particles in the coating. It has been studied in past that residual stresses in coating influence adhesion, peeling, and delamination of the coating [12-17]. In general, residual stresses are introduced in cold sprayed coating during deposition, when high-velocity powder particles plastically deform upon impact on the substrate or pre-deposited powder particles. These residual stresses, also called peening stresses, are predominately compressive in nature. In order to improve coating performance, it is very important to understand, predict and control internal stresses in the coatings. There are few numbers of studies has been performed analytically and experimentally to understand the generation of residual stresses in cold sprayed coating. Matejicek and Sampath [16] studied residual stresses in cold sprayed copper particles as a function of particles velocity and reported the resulting value of residual stresses of few tons of MPa at particles velocities ranging from 500 to 700 m/s. In this context, Luzin et al. [18] investigated residual stresses in copper/aluminum system by neutron diffraction and compared it with Tsui and Clyne's [17] progressive model to show that residual stresses were predominantly determined by plastic deformation at the high-velocity impact of particles with the negligible contribution of thermal stresses. Furthermore, Suhonen et al. [19] demonstrated the evolution of residual stress with respect of pretreatment of substrates in the case of Al, Cu and Ti coatings, deposited on aluminum and carbon steel substrates. They reported that the residual stresses are predominantly compressive in nature; however, the generation of residual stresses was also depending on the combination of coating and the

substrate materials. Arabgol et al. [20] analyzed the influence of geometry and material of coating/substrate system on the distortion and so on residual stresses introduced in cold sprayed coating by using finite element analysis.

There are a number of methods applied to determine the residual stresses in thermal sprayed and cold sprayed coatings e.g. neutron diffraction, X-ray diffraction, multilayer recursive matching, bending, and hole-drilling. Every technique has their own advantages and disadvantages [21]. Particularly, in the case of cold sprayed coating mainly neutron diffraction and X-ray diffraction methods have been used till now [18, 22]. These techniques are nondestructive techniques and can provide high spatial resolution with high sensitivity towards phase and structure of investigating material. However, the availability and quickness of these techniques are rather low in comparison to other techniques e.g. hole-drilling and bending techniques. Schonen et al. [19] used in-situ residual stress measurement in cold sprayed Al, Cu, and Ti coatings.

Numerous studies have been made for cold sprayed soft materials such as Aluminium [9, 23, 24], Copper [25, 26], Titanium [27, 28], and Tantalum [29]. However, high-temperature aerospace materials, such as Ni-based superalloys, are always a challenge to process by cold spray due to the high critical velocities and technical issues like nozzle clogging [30-33]. Ni-based superalloys e.g. Inconel IN 718 is one of the most demanding material in aerospace industries due to its high-temperature ductility and excellent corrosion resistance at elevated temperature. Ni-based superalloys e.g. Inconel 718 [32] and Inconel 625 [22] have been successfully processed by cold spray with helium as a processing gas. There are a very little number of studies available on Ni-based superalloys, especially on Inconel 718, where the material is successfully deposited by using nitrogen as an only processing gas [33-36]. Furthermore, investigation of residual stress generation and its influence on adhesion strength in Ni-based superalloys are still devoid. Recently, a single study for determination of residual stresses has been made by Srinivasan et al. [22] in cold sprayed Inconel 625 by using X-ray diffraction method.

The current study focused on determination of residual stresses in Inconel 718, sprayed by using nitrogen as a processing gas with Kinetics-8000, which has the water cooled nozzle to delay the nozzle clogging. Influence of coating thickness on the residual stress development was studied by using hole-drilling and bending method. A model for residual stress development in shot-peening is used to estimate the maximum residual stress in the coatings. Furthermore, the

combined influence of coating thickness and residual stress on the bond-strength has been investigated. A strain energy release criterion has been used to interpret the bond-strength results with the variation of coating thickness.

2. Experimental Details

2.1 Sample preparation

IN 718 powders (Oerlikon-Metco, Troy, MI, USA) with spherical morphology and mean particle size of 14 µm was used as feedstock powder. More details about powder are mentioned in our previous work [35].

IN 718 substrates with disc shape (3 mm thick and 30 mm in diameter) were used to prepare the specimen for residual stress measurements and microstructure analysis. Substrates with a diameter of 25 mm and thickness of 5.5 mm were deposited for coatings bond-strength test. These substrates were grit blasted with commercially available alumina grit with an average particle size of 420-600 µm prior to deposition. The average substrate roughness of R_a (≈3.1 µm) was evaluated by using an optical profilometer (Model CT350T, cyberTECHNOLOGIES GmbH, Germany).

Cold-sprayed IN 718 coatings were produced by using Nitrogen as the propellant gas with CGT-Oerlikon Metco Kinetics® 8000 high-pressure cold spray system equipped with the standard water-cooled D-24 de-Laval type converging-diverging nozzle. Water cooling of the nozzle can delay the nozzle clogging. Inlet gas pressure and temperature were 4 MPa and 950 °C, respectively. The stand-off distance from the nozzle exit to the substrate surface was 80 mm. A gun traverse speed of 500 mm/s was used for the coating deposition with the spray-angle of 90°. Coating thickness was varied by varying the number of deposition passes in range of 2 passes to 13 passes.

2.4 Characterization

Microstructure observations on as-polished coating cross-sections were performed by using Merlin FE-SEM, Carl Zeiss NTS GmbH, Oberkochen, Germany, in the backscattered electron imaging (BSI) mode. SEM-BSI micrographs with image analysis software (analySIS Pro, Olympus Soft Imaging Solutions GmbH) were used to evaluate coating porosity.

Furthermore, Microindentation tests were carried out at 16- points along the polished coating cross-sections to measure Vickers hardness and Young's Modulus of the coatings. Individual

measurements were done with an applied load of 100 g ≡ 1 N for 20 s by using microindentor (Fischerscope ® H100C, Helmut Fisher GmbH+Co, Germany) at Institute of Energy and Climate Research (IEK-2), Forschungszentrum Jülich GmbH. Indentation curves (unloading-displacement) were used to extract the value of the Young's Modulus.

Coating bond-strength test was performed on the tensile rig as per the European standard test method DIN: EN 582, [37]. A tensile load was applied to bonded cylindrical stems, using a constant rate of 1 mm/s, until fracture occurred and the amount of force required for separation was recorded. Bond-strength was determined as the maximum load divided by the cross-sectional area of the specimen. The coated specimen was examined after failure, and failure mode was identified if the coating failed internally (cohesive failure), the coating separated from the substrate (adhesive failure), or the coating remains intact with the substrate and the epoxy between the specimen and stems failed.

Residual stresses in cold sprayed IN 718 coating was evaluated by bending and hole-drilling methods. Bending method is based on curvature variation in the substrate before and after deposition. Bending of the substrate during deposition occurs due to the development of residual stress, which leads the substrate to curve. Curvature measurements were performed on the same specimen prior to deposition and after the coating deposition, by using optical profilometer (Model CT350T, cyberTECHNOLOGIES GmbH, Germany). Residual stress was determined by curvature change in the substrate-coating system by using Atkinson's equation [38, 39] –

$$\sigma_r = \frac{EH^2\kappa}{6h(1-\vartheta)(1+h/H)} \quad (1)$$

where, σ_r is the residual stress in the coating with thickness h, which causes a curvature change of κ. E is Young's modulus, υ is Poisson's ratio of the substrate, and H is the thickness of the substrate.

The residual stress depth profiles within the coatings and the substrates were evaluated using the incremental hole-drilling method (39-41). For the application of the incremental hole-drilling technique, a blind hole is incrementally drilled into the material while the strain release on the surface is measured using strain gauges. From the measured strain relaxations, the corresponding residual stresses are calculated on the basis of calibration data and the materials elastic constants. The incremental hole-drilling was carried out using a self-constructed drilling device and a TiN

cement carbide tool with a nominal diameter of 1.6 mm. The strain relaxations were determined using strain gage rosettes of type CEA-06-062UM-120, while each individual strain gauge was connected to a carrier frequency amplifier, type Picas, by Peekel Instruments GmbH (Bochum, Germany) via a half bridge (Wheatstone bridge) circuit with temperature compensation.

3. Results and Discussion

3.1 Microstructure

The coatings of IN 718 powder on IN 718 substrates, with 6 different coating thicknesses, were produced by using parameters, describes in section 2.1. All coating with six different coating thicknesses showed the typical cold sprayed microstructure of IN 718 coatings on IN 718 substrates, as reported in our previous work [35]. The microstructures of the coatings with two extreme coating thicknesses are shown in Fig. 1. Macroscopically, both coatings are uniform and free of large voids and cracks. Porosity evaluation of all 6 coatings with different coating thicknesses was performed by image analysis method and values are listed in Table 1. It can be observed that the overall porosity of IN 718 coating on IN 718 substrate is less than ~ 2% i.e. very dense (density ~98%) IN 718 coatings can be obtained by using nitrogen as a propelling gas.

3.2 Mechanical Properties

Young's modulus and Vickers hardness of coatings were measured as a function of coating thicknesses by using micro-indentation tests. Measured values of Young's modulus and Vickers hardness of as-sprayed IN 718 coatings on IN 718 substrate are given in Table 1. It has been observed that Young's modulus of IN 718 coatings show a linear behavior with coating thickness, as shown in Fig. 2 and increases with increase in coating thickness. Furthermore, Vickers hardness shows a slight increment with the increase in coating thickness; however, within the error limit, it is more or less constant. It indicates the effect of peening in the cold spray process where powder particle deforms partly by its own impact and partly by bombardment of upcoming powder particles. Peening effect increases with increase in coating thickness due to the addition of more number of impacting particles, as a consequence Young's modulus and hardness values increase. The deviation of mechanical properties from those of bulk material is mainly influenced by splat like microstructure, which leads to imperfection in the intersplat bonding, oxidation at splat surface, and to some extent porosity of the coating.

However, the microstructure of present cold sprayed IN 718 coatings suggests a very dense granular like microstructure with unobservable oxidation of the coating material. The quantitative values of Young's modulus and Vickers hardness of IN 718 coatings measured by micro-indentation tests are close to Young's modulus and Vickers hardness of bulk IN 718 material, as mentioned in Table 1.

3.3 Effect of coating thickness on Residual Stress

3.3.1 Residual stress evaluation by curvature measurement

The in-plane residual stresses were estimated by bending method, which evaluates the stress induced curvature of the substrate. The curvature introduced in the substrates was measured before and after the deposition of coatings by using optical profilometer. Grit blasting on IN 718 substrates was performed prior to deposition and effect of grit blasting on the bending of substrates i.e. on curvature measurement was subtracted from curvature measurement after the deposition of the coating. The first set of curvature measurements were performed on 6 specimens of different coating thickness ranged from 216 μm to 1173 μm, as mentioned in Table 2. Curvature development in the substrates shows a linear relationship with coating thickness, as shown in Fig 3a and given by a linear fit as follows-

$$\kappa = 212\,h + 22.6 \tag{2}$$

Residual stress evaluation of as-sprayed IN 718 coatings with variation of the coating thicknesses was carried out by using Atkins approach as mentioned in section §2.4 in Eq. 1, where, Young's modulus of E = 200 GPa and poisons ratio of $\upsilon = 0.29$ of the IN 718 substrate, and the thickness of the substrate of H = 3.0 mm. Change in the curvature before and after deposition of coatings with different coating thickness is given in Table 2. Fig. 3b illustrates the residual stress profile with respect to coating thickness.

The residual stress variation with coating thickness demonstrates the high value of compressive residual stresses in the coatings. However, it is possible to deposited thick coating (more than 1 mm) without spallation, peeling-off, and cracks. Moreover, it represents that coating thickness significantly influence the residual stress in the coating and it decreases with increase in coating thickness.

The second set of curvature measurements were performed on a single substrate with the successive increment of coating thickness in four steps, where deposition process was interrupted after each step followed by curvature measurement. Four residual stress values were successfully evaluated by measuring curvature after deposition of 148 μm, 300 μm, 548 μm, and 770 μm coating thicknesses in four steps. Residual stresses introduced in the coating with the increment of coating thickness are shown in Fig. 4. These results indicate that residual stress introduced in the coating are compressive in nature and decreases with increase in coating thickness up to 548 μm on the same substrate and when the coating thickness increases to more than 548 μm, these stresses were relaxed by peeling the entire coating from the substrate, as shown in photos taken after each successive deposition in Fig 4. These results clearly show the effect of peening during deposition, when deposition has been performed in a single run; it is possible to deposit more than 1 mm coating (Fig. 2b). However, if the deposition is interrupted i.e. peening is interrupted; it leads to relaxation of existing residual stresses in the coating by peeling off the entire coating from the substrate. It suggests that in spite of using the same substrate for deposition, after each step of the deposition coating/substrate system behave differently.

Fig. 4 and Fig. 5 demonstrate that at lower coating thickness (e.g. at 216 μm and at 148 μm) residual stresses in the coatings are exceptionally high due to the high curvature introduced into the substrate. The high curvature value (Fig. 4) at the lower coating thickness might be the combined effect of curvature introduced in the substrate due to the bombardment of high energy particles and curvature introduced due to the residual stress of the coating. It is hard to differentiate these two contributions to the curvature and the resultant value of curvature was used to calculate the residual stress. Therefore, the residual stress values are very high at lower coating thicknesses. Furthermore, in cold spray process, high-velocity particle deforms plastically during its impact upon the substrate or already deposited particle which means the final deformed state of the particle is the result of not just the initial impact, but also the successive particle impacts as the coating built up. This phenomenon induces compressive stress in the coating, causing the peening effect. The peening effect of bombarding particles accumulates with repeated impacts i.e. higher the coating thickness deposited by cold spray more will be peening effect and as a consequence, residual stresses should increase. However, as the coating built up, impact stress starts to relax either during or immediately after impact process through recovery and recrystallization. Dynamic recovery and recrystallization are expected to

relax the stress state. This might be the reason of decrease in residual stresses with the increase in coating thickness. However, to understand the recovery process a detailed quantitative study of dislocation density and spatial arrangements are required.

3.3.2 Depth profile of residual stresses by hole-drilling method

The incremental hole-drilling method was used to obtained depth profile of residual stresses in coatings and substrates. Specimen for the incremental hole-drilling test was deposited with the same parameters as specimens deposited for curvature measurements. Residual stress depth-profiles for two coating thicknesses were measured and corresponding data is plotted in Fig. 5. Residual stress depth-profiles demonstrate the compressive nature of residual stress in coatings while it turns to tensile in the substrate. It is also notable that residual stress gradually decreases from coating surface to interface (marked as the red and blue line in Fig. 5) after that a tensile peak appear in the substrate to balance the total stress of the system. Overall residual stress at the interface might be the combined effect of compressive and tensile stresses in the coating and in the substrate, respectively. However, residual stress profiles measured by bending method (Fig. 4) and by hole-drilling method (Fig. 5) suggest different behavior of residual stress with respect to coating thickness. The hole-drilling method reveals that residual stress decreases in depth from coating surface to the coating/substrate interface while bending method suggests that overall residual stress clearly decreases with increase in coating thickness. This contradictory behavior can be explained as the incremental hole-drilling method measured the distribution of residual stress in single coating/substrate system with particular coating thickness, whereas curvature measurement measures a mean coating stress and has been applied on different coating/substrate systems with different coating thicknesses. Therefore for better comparison residual stress distribution in single coating/substrate has been estimated by Tsui and Clyne's progressive deposition model and explained in detail in the next section.

3.3.3 Estimated stress distribution in cold sprayed IN 718

The distribution of residual stress throughout the coating/substrate system was estimated from Tsui and Clyne's progressive deposition model [13, 17]. Residual stress at the surface of the coating, at the interface and at the bottom of the substrate is given by:

$$\sigma_{c\,(at,\ z=h)} = -\frac{F}{bh} + E_c \cdot \Delta\kappa \cdot (h - \delta) \tag{4}$$

$$\sigma_{c\,(at,\ z=0)} = -\frac{F}{bh} + E_c \cdot \Delta\kappa \cdot \delta \quad (5)$$

$$\sigma_{s\,(at,\ z=0)} = \frac{F}{bH} - E_s \cdot \Delta\kappa \cdot \delta \quad (6)$$

$$\sigma_{s\,(at,\ z=-H)} = \frac{F}{bH} - E_s \cdot \Delta\kappa \cdot (H + \delta) \quad (7)$$

Where, the first term in Eq. (4-7) is the residual stress due to strain mismatch and the second term is the bending contribution, which originates from the curvature change *Δκ*. *F* is the force applied on coating/substrate system to remove strain misfit, b is the width of the substrate, and δ is the distance from the neutral axis. A pair of equal and opposite forces, due to strain misfit, acts on coating/substrate system and generate a bending moment. On the basis of force and momentum balance, *F*/*b* and δ is given by [13, 17]:

$$\frac{F}{b} = \Delta\varepsilon \left(\frac{hE_c \cdot HE_s}{(hE_c + HE_s)}\right) \quad (8)$$

$$\text{where, } \Delta\varepsilon = \frac{\Delta\kappa(E_c^2h^4 + 4E_cE_sh^3H + 6E_cE_sh^2H^2 + 4E_cE_shH^3 + E_s^2H^4)}{6E_cE_s(h+H)hH} \quad (9)$$

$$\delta = \frac{h^2E_c - H^2E_s}{2(hE_c + HE_s)} \quad (10)$$

In thermally sprayed coating, residual stresses develop due to quenching stress (rapid cooling and solidification of molten droplets) and the thermal stress (difference in coefficient of thermal expansion of coating and substrate material). Therefore, misfit strain is mainly due to the temperature change of coating/substrate system. Whereas, in cold sprayed coating, the possible source of misfit strain is (a) deformation induced stresses during the impact of the powder particles at the substrate or previously deposited particles (b) cooling stress due to different coefficient of thermal expansion of coating and substrate material. When coating and substrate material are the same, i.e. similar to the present study, IN 718 powder material on IN 718 substrate, misfit strain can be related mainly to deformation induced stresses [20]. It has also been assumed that powder particle and substrate are at the same temperature during deposition. Ec = Es = E/(1-υ) was used to estimate the residual stress distribution in the coating/substrate system. Eqs. (4-10) can be re-written with Ec = Es = E/(1-υ):

$$\sigma_{c\,(at,\ z=h)} = -\frac{F}{bh} + \frac{E \cdot \Delta\kappa \cdot (h-\delta)}{(1-\upsilon)} \quad (11)$$

$$\sigma_{c\,(at,\ z=0)} = -\frac{F}{bh} + \frac{E\cdot\Delta\kappa\cdot\delta}{(1-\upsilon)} \tag{12}$$

$$\sigma_{s\,(at,\ z=0)} = \frac{F}{bH} - \frac{E\cdot\Delta\kappa\cdot\delta}{(1-\upsilon)} \tag{13}$$

$$\sigma_{s\,(at,\ z=-H)} = \frac{F}{bH} - \frac{E\cdot\Delta\kappa\cdot(H+\delta)}{(1-\upsilon)} \tag{14}$$

$$\frac{F}{b} = \Delta\varepsilon\left(\frac{hHE}{(h+H)\cdot(1-\upsilon)}\right) \tag{15}$$

$$\Delta\varepsilon = \frac{\Delta\kappa(h+H)^3}{6hH} \tag{16}$$

$$\delta = \frac{h-H}{2} \tag{17}$$

The estimated stress values are listed in Table 3. Fig. 6 shows the estimated stress distribution throughout the coating/substrate system for different coating thicknesses ranged from 216 µm to 1173 µm. The stress distribution, estimated by Tsui and Clyne's progressive model, shows that stress increases from coating surface to interface, while experimentally measured stress distribution by hole-drilling method demonstrates the opposite behavior i.e. stress decreases from coating surface to interface. This contradictory behavior might be due to stress relaxation via dynamic recovery and recrystallization in cold sprayed coatings during or after the deposition. Coating layers near to interface experienced more work hardening as compared to the surface layer due to the successive bombardment of particles i.e. inner layers store more strain energy, as a consequence stress accumulation might be higher in the layers near to the interface. It is known for thermal spray coatings that the stresses induced due to thermal misfit in the coating/substrate system has a limit to accommodate it elastically and beyond this limit, it accommodates through inelastic mechanisms, such as, cracks, peeling-off the coatings, sliding, and creeping etc. [18]. Similarly, in the case of cold spray process stresses must have the certain limit to accommodate in the coating/substrate system and beyond that limit; it might also relax via some inelastic mechanisms. However, it has been observed that there were no cracks and peeling-off defects present in the coatings which indicate that the excess stored strain energy acts as driving force to relax the stresses via dynamic recovery and recrystallization. It implies that due to higher accumulation of stresses, stress relaxation might also be higher in inner layers, which results in the decrease in the resultant residual stress i.e. residual stress decreases from coating surface to the interface. Stress relaxation has not been considered in the Tsui and Clyne's progressive

model for stress distribution while experimentally measured stress distribution demonstrates the actual state of stress within the layers. However, the residual stress interpretation in cold sprayed coatings is less straightforward due to the complexity of the process and not enough knowledge about multiple modes of stress relaxation, non-uniform deformation, and recrystallization [18]. A different approach has been used to estimate average residual stress in cold sprayed coatings by using physical process parameters in next section.

3.3.4 Estimated residual stress in cold sprayed IN 718 coating

To estimate the theoretical value of residual stresses in IN 718 coating, a modified model of residual stress accumulation in the shot peening process has been used, which is based on Hertzian contact and assumed that plastic deformation on loading-unloading developed in shot peening process [43-45], similar to the cold spray coatings. More details about this approach have been given in reference [18] where Luzin et al. applied a similar approach to estimate residual stress, generated in cold-sprayed Cu and Al coatings. In the cold spray process particles partly deform by its own impact, and partly by the successive particles to build up the coating. The assumption in the model is that final amount of deformation is more significant than successive deformation.

The maximum residual stresses at the surface can be given as [18, 44]

$$\sigma_e = -(0.333 + 0.286\alpha\beta)(1 - \alpha\beta)[(1 - 2\alpha\beta)\sigma_s + k \cdot \alpha\beta \cdot p_{max}] \quad (18)$$

$$p_{max} = \frac{2}{\pi}\left(\frac{5}{4}\,\pi E_{eq}^2 \rho v^2\right)^{1/5} \quad (19)$$

Where, σ_s is the yield stress, k is a constant close to 1. $\alpha\beta$ is coupled parameter based on the elastoplastic state of deformed material, where α is the simply ratio of strain hardening rate to Young's modulus and β is the ratio of the true plastic strain to true elastic strain. p_{max} is the maximum pressure at impact stress, ρ is the density of the material, v is the impact velocity of the particle, E_{eq} is the equivalent modulus, given as $E_{eq} = E/(1-\upsilon)$.

The process parameters mentioned in Table 4 is used to calculate the maximum residual stress by using Eq. 18. These parameters were estimated on the basis of linear momentum transfer on impact. The impact velocity of the particle was estimated by using kss solution software for a given particle size distribution [46]. The impact strain was calculated by the change of aspect ratio from sphere to ellipsoid after deformation. The aspect ratio for spherical IN 718 powder

particle was calculated by fitting the SEM micrograph, (as published in our previous work [35]) of the deformed particle to an ellipsoid. Impact duration was simply estimated with the assumption that particle velocity decreases linearly, which also gives the average strain rates. Steenkiste et al. [47] used the approach of momentum transfer over the calculated impact time to calculate the average impact pressure in case of cold sprayed Al- coatings; the similar way has been used in the present study to calculate average impact pressure during the impact of IN 718 powder particle on IN 718 substrate. Furthermore, maximum impact pressure (P_{max}) was calculated by using Eq. 19. For the given impact velocity the value of P_{max}, mentioned in Table 4, is beyond the Hugoniot elastic limit of 1.2 GPa for IN 738 material [48]. The exact value of the Hugoniot elastic limit IN 718 material is not available, it has been assumed to be close to the Hugoniot elastic limit of IN 738 material. Hence to calculate maximum residual stress at the surface, an average impact stress has been used in place of P_{max}. The estimated value of σ_{max} of 240 MPa has been compared with the average residual stress measured by hole-drilling and bending method. Although the estimated value of residual stress is a rough estimation and has not considered the influence of coating thickness yet it has good agreement with measured residual stress values for the coating thickness of ~ 600 μm, as mentioned in Table 5. The exact estimation of residual stress in cold spray process is not very straightforward as it might also be influenced by dynamic and static recovery, strain rate sensitivity and particle size.

3.4 Effect of coating thickness on adhesion-strength of the coatings

Variation of adhesion-strengths of IN 718 coating with different coating thicknesses was evaluated by the bond-strength test. Three specimens were tested for each coating thickness and the average bond-strength values with standard deviation are listed in Table 6. Fig. 7a shows that the adhesion-strength between coating and substrate decreases with increasing coating thickness. It can also be observed that bond-strength value of higher coating thickness (more than 650 μm) is rather low, although the potential capabilities of cold spray process to deposit thick coatings with compressive residual stresses. These strengths can be improved by heat treatments; however, the present study is fully devoted to studying the properties of as-sprayed IN 718 coatings on IN 718 substrates by cold spray process for maintenance, repair, and operation (MRO) applications of large aero engine components. The focus of bond-strength tests was to elucidate the adhesion strength between coating and substrate, although few failures at lower coating thicknesses (at 146 μm and 284 μm) occurred partly at the interface between coating and

substrate and partly between glue and the coating, as shown schematically in Fig. 7b. Actual photos of failures in Fig. 8 indicate that the area of interface failure increases with increase in coating thickness. Furthermore, mixed mode failure of two coatings (thickness 146 μm and 284 μm) indicates the high adhesion strength at the interface between coating and substrates, which might be due to exceptionally high compressive residual stress in the coating, as evaluated by bending method for lower coating thickness. The depth-profile of residual stress in Fig. 6 suggests that compressive residual stress progressively decreases towards the substrate up to zero and further tensile stresses appear to balance the total stress in the coating-substrate system. Stress at interface might be affected by resultant compressive stress in the coating and the substrate.

A fracture mechanics approach was applied based on the energy-release-rate criterion for debonding. The energy-release-rate is the amount of energy released for a unit area of the crack surface created if the crack (or debonded region) were to grow. When the energy-release-rate reaches a critical value, G_c, crack extension or further debonding occurs. The energy-release-rate criterion has also been applied to predict fracture and debonding in past [49, 50]. The energy-release-rate criterion is applicable to the cases with little plasticity, which is the case of cold sprayed coatings were sprayed material has very low ductility due to the high intensity of work hardening. It has been observed that debonding is not only influenced by the residual stresses of the coating but also the external mechanical load applied during the mechanical testing [51-53]. In the present case, net energy-release-rate (G_t) on debonding is considered to be the sum of the energy-release- rate due to residual stresses (in-plane stress) in the coating (G_r) and the energy-release-rate due to externally applied stress (out-plane stress) (G_a). The energy-release-rate due to externally applied stress can be written as:

$$G_a = \frac{\sigma_a^2(\pi a)(1-\vartheta)}{E} \quad [54, 55] \tag{20}$$

where σ_a is the externally applied stress, a is the crack length.

The strain energy release rate due to residual stresses for planar geometry is given by:

$$G_r = \frac{\sigma_r^2 h(1-\vartheta)}{2E} \quad [51] \tag{21}$$

where σ_r is the average residual stress in the coating, h is the coating thickness.

The net strain energy release rate is estimated by the sum using Eq. 6 and Eq. 7-

$$G_t = G_a + G_{\mathrm{r}} \tag{22}$$

$$G_t = \frac{\sigma_a^2(\pi a)(1-\vartheta)}{E} + \frac{\sigma_r^2 h(1-\vartheta)}{2E} \tag{23}$$

With the failure criterion, $G_{\mathrm{t}} = G_{\mathrm{c}}$, the external applied stress can be written as:

$$\sigma_a = \left[\frac{E}{(1-\vartheta)\cdot c}\left\{G_{\mathrm{c}} - \frac{\sigma_r^2 h(1-\vartheta)}{2E}\right\}\right]^{1/2} \text{ where, } c = \pi a \tag{24}$$

The experimentally measured bond-strength profile with respect to coating thickness (Fig. 8) was used as input data to fit with the predicted bond-strength profile, obtained by using Eq. 10, where, G_{c} and c have been consider as the fitting parameter. These calculations are based on the assumption that residual stress is constant for all coatings. The estimated value of residual stress of 240 MPa is used for the calculations.

The solid curve in Fig. 9 shows the predicted bond-strength profile with respect to coating thickness. The comparison of predicted and measured values of bond-strength for specific coating thickness, along with the estimated value of the critical energy-release-rate and crack length, is listed in Table 5. The predicted values of bond-strengths are close to the measured bond-strength values at different coating thicknesses. Furthermore, the predicted bond-strength profile with respect to coating thickness demonstrates the similar behavior as measured bond-strength profile i.e. the bond-strength values decrease with increase in coating thickness. However, in the absence of residual stresses i.e. $\sigma_{\mathrm{r}} = 0$ MPa, bond-strength is independent of coating thickness, as shown in Fig. 9 by the black line. It suggests that a residual stress in the coatings is required to predict the observed reduced bond-strength for increasing coating thickness i.e. residual stress in the coating influences the bond-strength between the coating and the substrate. Although, the estimated crack length (from fitting) is higher than then the coating thickness yet it helps to provide a degree of confidence in the basic validity model. An in-depth estimation of facture mechanical behavior has to take into account the actual geometry of the existing defects, which will be beyond the scope of the present work.

Conclusion

The influence of coating thickness on residual stress and bond-strength was studied in cold sprayed IN 718 coatings on IN 718, deposited by using N_2 as a propelling gas. Mechanical properties of IN 718 coatings increase with the increase in coating thickness and approaches to bulk value of IN 718 material. Residual stresses in the coatings are compressive in nature and stress accumulation depends on peening during the deposition. Residual stress distribution indicates a possibility of residual stress relaxation via dynamic recovery and recrystallization during or just after the deposition. Average compressive residual stress decreases with increase in coating thickness. Bond-strength of the coatings also decreases with increase in coating thicknesses. The energy-release-rate criterion was used to predicted bond-strength with increasing coating thickness. The influence of residual stress on decreasing bond-strength was investigated. Predicted bond-strength values are close to the measured bond-strength values and decrease with increase in coating thickness in the presence of residual stresses in the coating. While it is independent of coating thickness when residual stresses are zero.

Acknowledgments

The authors greatly acknowledge the finical support by German Federal Ministry of Economic Affairs and Energy (Bundesministerium für Wirtschaft und Energie) under grant number – 20T1317B. The authors would like to thanks to Mr. Karl-Heinz Rauwald for supporting in coating deposition and Mr. Mark Kappertz for metallographic preparation of deposited samples. Authors also would like to thank Dr. Robert Mücke and Dr. Markus Mutter for fruitful discussion on this topic.

References

[1] A. Papyrin, V. Kosarev, K.V. Klinkov, A. Alkhimov, V. K. Fomin, Cold Spray Technology, Elsevier Ltd., Oxford, 2006.

[2] V.K. Champagne, The Cold Spray Deposition Process: Fundamentals and Applications, Woodhead Publishing Ltd., Cambridge, 2007.

[3] T. Stoltenhoff, H. Kreye, H.J. Richter, An Analysis of the Cold Spray Process and Its Coatings, J. Therm. Spray Technol. 11(2002) 542-550.

[4] R. Dykhuisen, M. Smith, Gas Dyanamic Principle of Cold Spray, J. Therm. Spray Technol. 7(1998) 205-212.

[5] V.K. Kosarev, S.V. Klinkov, A.P. Alkhimov, A. Papyrin, On Some Aspects of Gas Dynamics of the Cold Spray Process, J. Therm. Spray Technol. 12 (2003)265-281.

[6] T. Schmidt, H. Assadi, F. Gärtner, H. Richter, T. Stoltenhoff, H. Kreye,T. Klassen, From Particle Acceleration to Impact and Bonding in Cold Spraying, J. Therm. Spray Technol. 18 (2009)794-808.

[7] J. Pattison, S. Celotto, R. Morgan, M. Bray, W. O'Neill, A Non-Thermal Approach to Freeform Fabrication, Int. Mach. Tools Manug., 47 (2007) 627-634.

[8] K. Spencer, V. Luzin, N. Matthews, M. Zhang, Residual Stresses in Cold Spray Al Coatings:The Effect of Alloying and of Process Parameters, Surf. Coat. Technol., 206 (2012) 4249-4255.

[9] K. Balani, T. Laha, A. Agarwal, J. Karthikeyan, N. Munroe, Effect of Carrier Gases on Microstructural and Electrochemical Behavior of Cold-Sprayed 1100 Aluminum Coating, Surf. Coat.Technol., 195 (2005) 272-279.

[10] H. Koivuluoto, J. Nakki, P. Vuoristo, Corrosion Properties of Cold-Sprayed Tantalum Coatings, J. Therm. Spray Technol., 18 (2009) 75-82.

[11] W.B. Choi, L. Li, V. Luzin, R. Neiser, T. Gna, Integrated Characterization of Cold Sprayed Aluminum Coatings, Acta Mater., 55 (2007) 857-866.

[12] M. Buchmann, R. Gadow, J. Tabellion, Experimental and Numerical Residual Stress Analysis of Layer Coated Composites, Mater. Sci. Eng., A288 (2000)154-159.

[13] T.W. Clyne, S.C. Gill, Residual Stresses in Thermal Spray Coatings and Their Effect on Interfacial Adhesion: A Review of Recent Work, J. Therm. Spray Technol., 5(1996) 401-418.

[14] S. Sampath, X.Y. Jiang, J. Matejicek, L. Prchlik, A. Kulkarni, A. Vaidya, Role of Thermal Spray Processing Method on the Microstructure, Residual Stress and Properties of Coatings: an

Integrated Study for Ni-5 wt.%Al Bond Coats, Mater. Sci. Eng., A364 (2004) p 216-231

[15] P. Bansal, P.H. Shipway, S.B. Leen, Residual Stresses in High-Velocity Oxy-Fuel Thermally Sprayed Coatings-Modelling the Effect of Particle Velocity and Temperature During the Spraying Process, Acta Mater., 55(2007) 5089-5101.

[16] J. Matejicek and S. Sampath, Intrinsic Residual Stresses in Single Splats Produced by Thermal Spray Processes, Acta Mater., 49 (2001)1993-1999.

[17] Y.C. Tsui and T.W. Clyne, An Analytical Model for Predicting Residual Stresses in Progressively Deposited Coatings—Part 1:Planar Geometry, Thin Solid Films, 306 (1997) 23-

[18] V. Luzin, K. Spencer, M.X. Zhang, Residual Stress and Thermo-Mechanical Properties of Cold Spray Metal Coatings, Acta Mater., 59 (2011)1259-1270.

[19] T. Schonen, T. Varis, S. Dosta, M. Torrell, J.M. Guilemany, Residual Stress Development in Cold Sprayed Al, Cu and Ti Coatings, Acta Mater., 61 (2013) 6329-6337.

[20] Z. Arabgol, H. Assadi, T. Schmidt, F. Gärtner, T. Klassen, Analysis of Thermal History and Residual Stress in Cold-Sprayed Coatings, J. Therm. Spray Technol., 23 (2014) 84-90.

[21] Schajer, G. S. 2013. Practical residual stress measurement methods, Chichester: Wiley.

[22] Dheepa Srinivasan, Vighnesh Chandrasekhar, Ramar Amuthan, Y.C. Lau, Eklavya Calla, Characterization of Cold-Sprayed IN625 and NiCr Coatings, J. Therm. Spray Technol., 25 (2016) 725-744.

[23] Y. Tao, T. Xiong, C. Sun, L. Kong, X. Cui, T. Li, G.L. Song, Microstructure and Corrosion Performance of a Cold Sprayed Aluminium Coating on AZ91D Magnesium Alloy, Corros. Sci., 52(2010) 3191-3197.
[24]. R. Morgan, P. Fox, J. Pattison, C. Sutcliffe, W. O. Neill, Analysis of Cold Gas Dynamically Sprayed Aluminium Deposits, Mater. Lett., 58(2004) 1317-1320.
[25] C. Li, W. Li, Y. Wang, and H. Fukanuma, Effect of Spray Angleon Deposition Characteristics in Cold Spraying, Thermal Spray 2003: Advancing the Science and Applying the Technology, 2003,p 91-96
[26]. H. Koivuluoto, ‘‘Microstructural Characteristics and Corrosion Properties of Cold-Sprayed Coatings,’’ Tampere University of Technology, 2010.
[27] T.S.S. Price, P.H.H. Shipway, and D.G.G. McCartney, Effect ofCold Spray Deposition of a Titanium Coating on Fatigue Behavior of a Titanium Alloy, J. Therm. Spray Technol., 2006, 15(4), p 507-512.
[28] C.-J. Li and W.-Y. Li, Deposition Characteristics of Titanium Coating in Cold Spraying, Surf. Coatings Technol., 2003, 167(2-3), p 278-283.
[29] H. Koivuluoto, J. Nakki, and P. Vuoristo, Corrosion Properties of Cold-Sprayed Tantalum Coatings, J. Therm. Spray Technol., 2009, 18(March), p 75-82.

[30] A.O. Tokarev, Structure of Aluminum Powder Coatings Prepared by Cold Gas dynamic Spraying, Met. Sci. Heat Treat. 38 (1996) 136-139.

[31] J. Karthikeyan, A. Kay, Cold Spray Technology: An Industrial Perspective, in: C. Moreau, B. Marple, (Eds.), Proceedings of Thermal Spray 2003: Advancing the Science & Applying the Technology, ASM International, Orlando, FL, p 117-121.

[32] T. Marrocco, D. McCartney, P. Shipway, A.J. Sturgeon, Comparison of the Microstructure of Cold Sprayed and Thermally Sprayed In718 Coatings, in: Marple, B., Hyland, M., Lau, Y.-C., Lima, R.S., Voyer, J., (Eds.), Proceedings for Thermal Spray 2006: Building on 100 Years of Success, ASM International, Seattle, WA.

[33] W. Wong, E. Irissou, P. Vo, M. Sone, F. Bernier, J.-G. Legoux, H. Fukanuma, S. Yue, J. Therm. Spray Technol. 22 (2013) 413-421.

[34] S. Bagherifard, G. Roscioli, M. Vittoria Zuccoli, M. Hadi, G. D’Elia, A. G. Demir, B. Previtali, J. Kondás, M. Guagliano, Cold Spray Deposition of Freestanding Inconel Samples and Comparative Analysis with Selective Laser Melting, J Therm Spray Tech (2017). doi:10.1007/s11666-017-0572-3.

[35] R. Singh, K. -H. Rauwald, E. Wessel, G. Mauer, S. Schruefer, A. Barth, S. Wilson and R. Vassen, Effects of substrate roughness and spray-angle on deposition behavior of cold-sprayed Inconel 718, Surface & Coatings Technology 319 (2017) 249–259.

[36] G. Mauer, R. Singh, K.-H. Rauwald, S. Schruefer, S. Wilson, and R. Vaßen, Diagnostics of Cold Sprayed Particle Velocities Approaching Critical Deposition Conditions, J. Therm. Spray Technol., DOI: 10.1007/s11666-017-0596-8, 2017.

[37] European standard, Determination of the Tensile Adhesive Strength of Thermally Sprayed Coatings, DIN: EN582, 1993.

[38] A. Atkinson, Br. Ceram. Proc. 54, 1 (1995).

[39] C.A. Klein, How accurate are Stoney's equation and recent modifications, J. Therm. Spray Technol. 88 (2000) p. no. 5487-5489.

[40] E. Obelode and J. Gibmeier, Influence of the Interfacial Roughness on Residual Stress Analysis of Thick Film Systems by Incremental Hole Drilling, Mater. Sci. Forum, 2014, 768-769, p 136-143

[41] N.J. Rendler and I. Vigness, Hole-Drilling Strain-Gage Method of Measuring Residual Stresses, Exp. Mech., 1966, 6, p 577-586

[42] E. Held and J. Gibmeier, Residual Stress Analysis of Thick Film Systems by the Incremental Hole-Drilling Method—Influence of Interlayers and Interfacial Roughness, HTM J. Heat Treatm. Mater., 2014, 69, p 71-79.

[43] Li JK, Mei Y, Duo W, Renzhi W. Mater Sci Eng A 1991;147:167.

[44] Ogawa K, Asano T. Mater Sci Res Int 2000;6:55.

[45] Franchim AS, Campos VSd, Travessa DN, Neto CdM. Mater Des 2009; 30:1556.

[46] https://kinetic-spray-solutions.com/kssapp/

[47] Van Steenkiste TH, Smith JR, Teets RE. Surf Coat Technol, 2002;154:237.

[48] E.B. Zaretskya, G.I. Kanelb, S.V. Razorenovc, K. Baumungd, Impact strength properties of nickel-based refractory superalloys at normal and elevated temperatures, International Journal of Impact Engineering 31 (2005) 41–54.

[49] D.J. Greving, J.R. Shadley, and E.F. Rybicki, Effects of Coating Thickness and Residual Stresses on the Bond Strength of ASTM C633-79 Thermal Spray Coating Test Specimens, J. Therm. Spray Technol., 3 (1914) 371-378.

[50] C.W. Marynowski, F.A. Halden, and E.P. Farley, Variables in plasma spraying, Electrochem. Technol., 3 (1965) 109-115.

[51] S.J. Howard, Y.C. Tsui, and T.W. Clyne, The Effect of residual stresses on the debonding of coatings, Part I: A model for deleamination at a biomaterial Interface, Acta Metall. Mater. 42 (1994) 2823-2836.

[52] M. Charalambides, AJ. Kinloch, Y. Wang and J.G. Williams, On the Analysis of Mixed Mode Faliutre, Int. J. Fract., 54 (1992) 269-291.

[53] T.W. Clyne and S.C. Gill, Residual Stresses in Thermal Spray Coatings and Their Effect on Interfacial Adhesion: A Review of Recent Work, J. Therm. Spray Technol., 5 (1996) 401- 418.

[54] W. Han, E.F. Rybicki, and J.R. Shadley, Application of Facture Mechanics to the Interpretation of Bond strength Aata from ASTM Standard C633-79, J. Therm. Spray Technol. 2 (1993) 235-241.

[55] E.F. Rybicki and M.F. Kanninen, A Finite Element Calculations of Stress Intensity Factors by a Modified Crack Closure Intergral, Eng. Frac. Mech. 9 (1977) 931-938.

Table 1: Experimental values of coating porosity and mechanical properties with variation of coating thickness

Young's modulus of bulk IN 718 material = 200 GPa, Vickers hardness – 496 HV			
Coating thickness (μm)	Porosity (%)	Young's modulus (GPa)	Vickers hardness (HV)
216	1.1±0.38	123±6	450±44
365	1.9±0.12	143±12	474±58
546	1.5±0.22	185±11	479±21
743	1.4±0.19	197±23	531±83
903	1.6±0.15	185±8	487±57
1173	0.7±0.25	197±9	508±40

Table 2: Parameters used to calculate residual stress by using Atkins's equation (Eq. 1)

Young's modulus of IN 718 substrate (E) = 200 GPa; Poisson's ratio for IN 718 = 0.29; Substrate thickness (H) = 3.0 mm		
Coating thickness (h) (μm)	Curvature change (κ) (m^{-1})	Calculated residual stress (σ_r) (MPa)
216	0.70767	-1291
365	0.35697	-368
546	0.36253	-237
743	0.41806	-191
903	0458	-165
1173	0.51737	-134

Table 3: Estimated residual stress values for coating/substrate system of varying coating thickness

Coating thickness (μm)	σ_c (at z = h) (MPa)	σ_c (at z = 0) (MPa)	σ_s (at z = 0) (MPa)	σ_s (at z = -H) (MPa)
216	-1270	-1868	+392	-206
365	-351	-652	+196	-106
546	-211	-517	+197	-110
743	-150	-503	+225	-129
903	-110	-498	+244	-143
1173	-57	-493	+274	-163

Table 4: Impact parameters estimated on the basis of linear momentum transfer on impact

Particle size (μm)	Density Kg/m^3	Yield Strength (MPa)	Impact speed (m/s)	Impact duration (s)	True impact strain	Average strain rate (s^{-1})	Average Impact pressure (MPa)	Maximum Impact pressure (GPa)	αβ
14	8190	725	744	1.88×10^{-8}	-0.26	1.38×10^{7}	756	113	0.005

Table 5: Estimated and experimentally measured residual stresses in cold sprayed IN 718 coatings

Estimated residual stress (MPa)	Residual stress calculated by bending method (MPa)	Residual stress measured by hole-drilling method (MPa)
-240	-245	-289

Experimentally measured residual stress with coating thickness ~ 600μm

Table 6: Adhesion-strength values of coating/substrates interface for different coating thicknesses

Coating thickness (µm)	Bond-Strength (MPa) (measured values)	Bond-Strength (MPa) (estimated values)
146	72.5±9.2	70.6
284	77±1.4	65.7
516	57±5.7	50.9
645	33.5±2.1	45.4
849	25.5±0.7	35.0
1081	17±2.8	16.3
With G_c = 340 J/m^2 and c = 0.006 m i.e. crack length, a = 0.002 m		

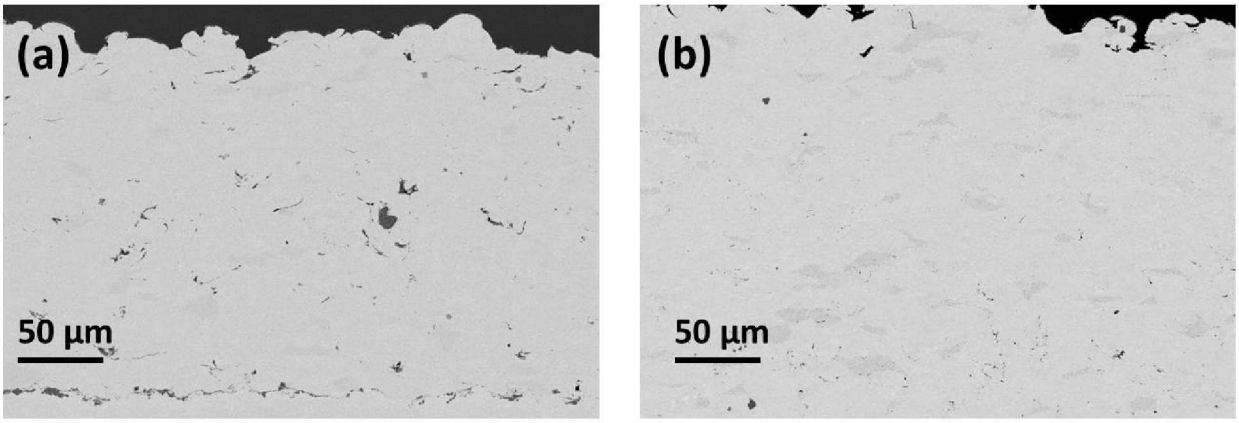

Figure 1: SEM micrograph of cold sprayed IN 718 coating on IN 718 substrate with coating thickness (a) 216 µm (b) 1173 µm

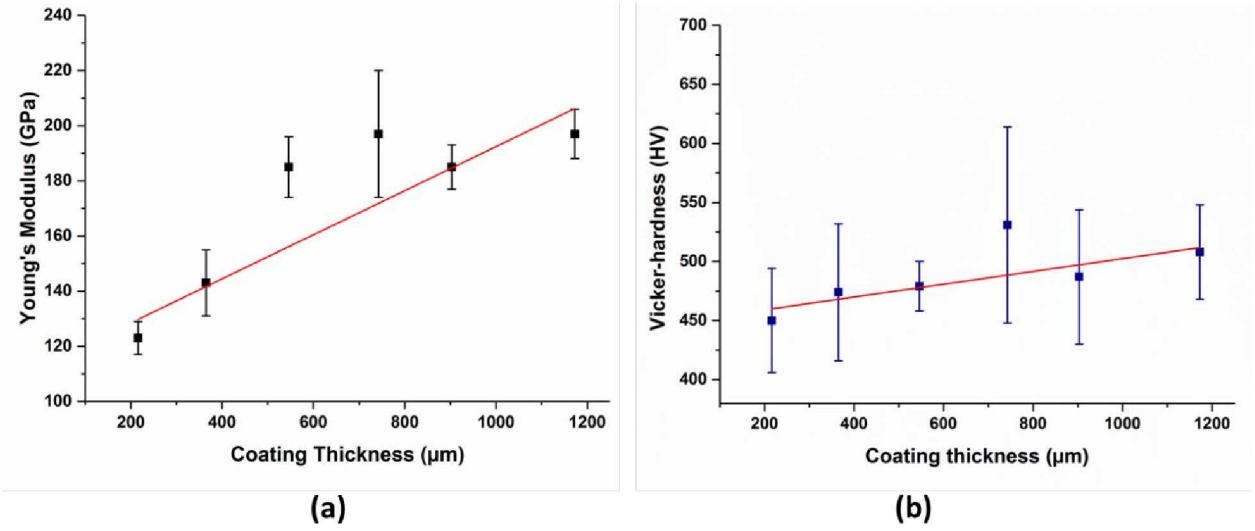

Figure 2: Mechanical properties of cold sprayed IN 718 on IN 718 substrate with variation of coating thickness (a) Young's modulus (b) Vickers hardness.

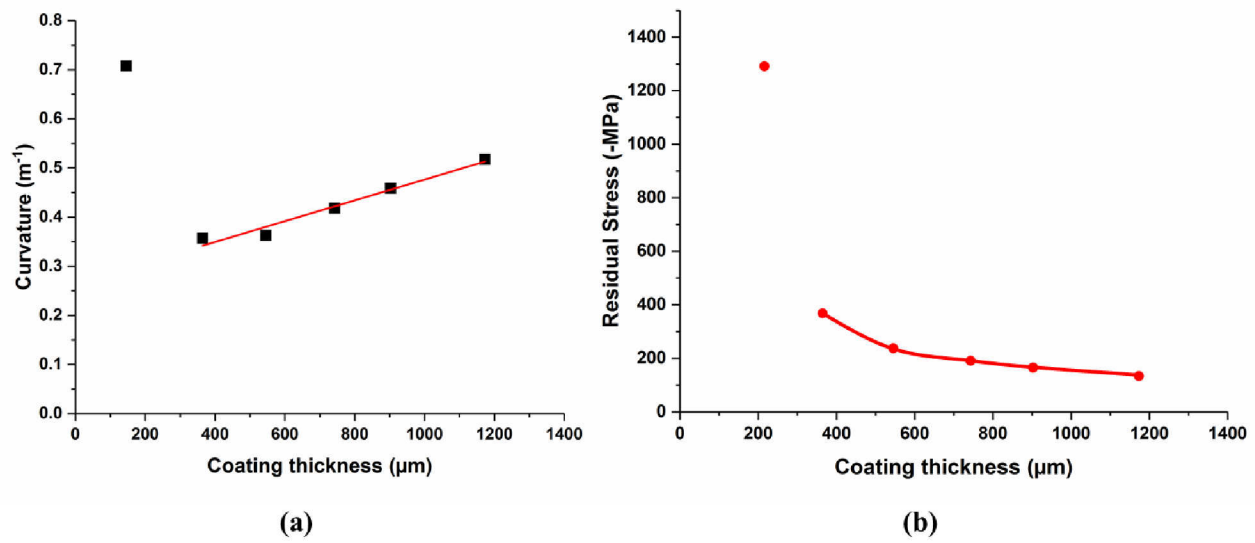

Figure 3: (a) Curvature change in the substrate after deposition of coating with different coating thickness (b) residual stress in the coatings of varying thickness, red line the guide line to follow the data points.

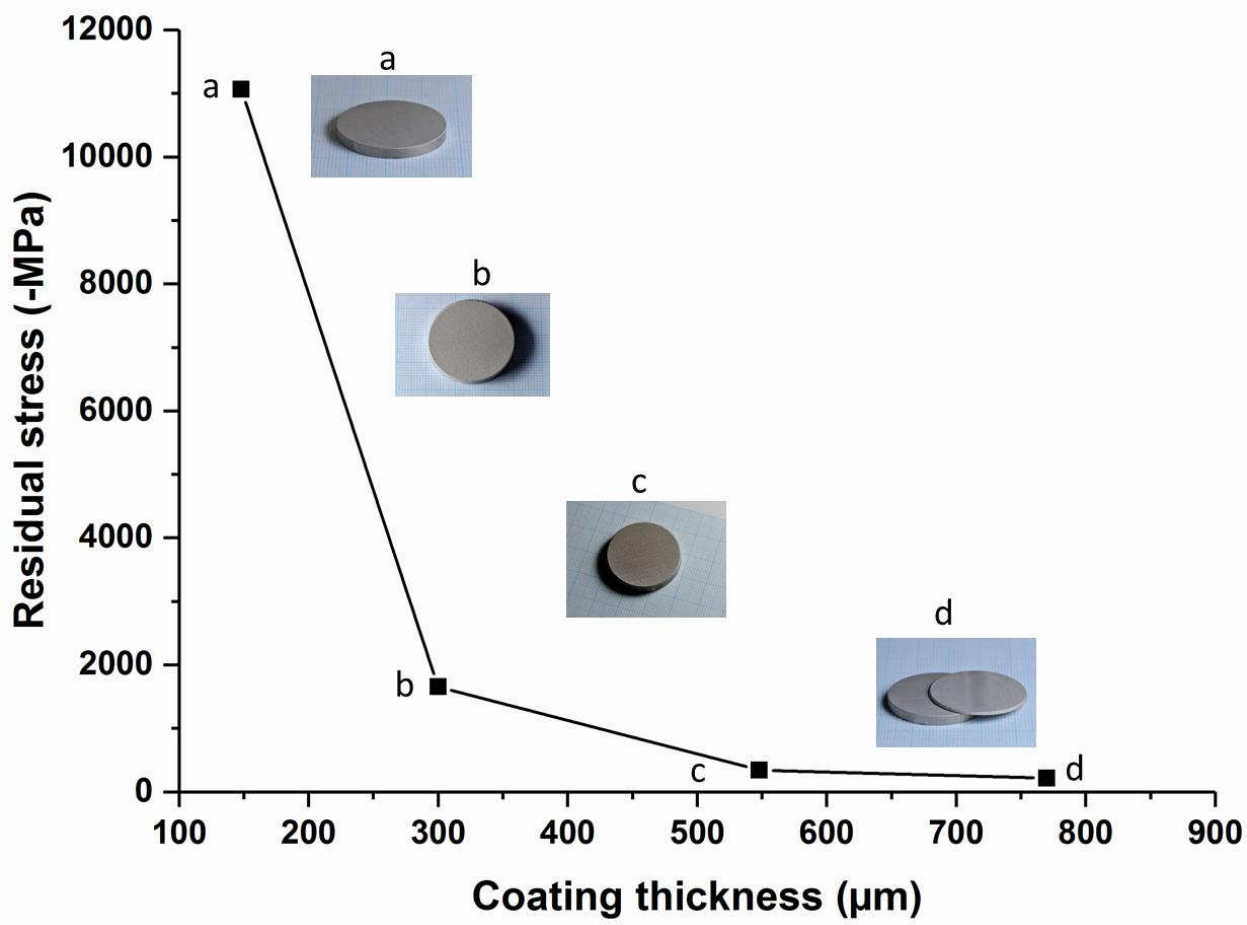

Figure 4: Residual stress profile measured by bending method with the increment of coating thickness in four steps. Photos of the as-sprayed coating of IN 718 powder on IN 718 substrate after depositing coating thickness of (a) 148 µm, (b) 300 µm, (c) 548 µm, and (d) 770 µm, where coating peeled out complete from substrate.

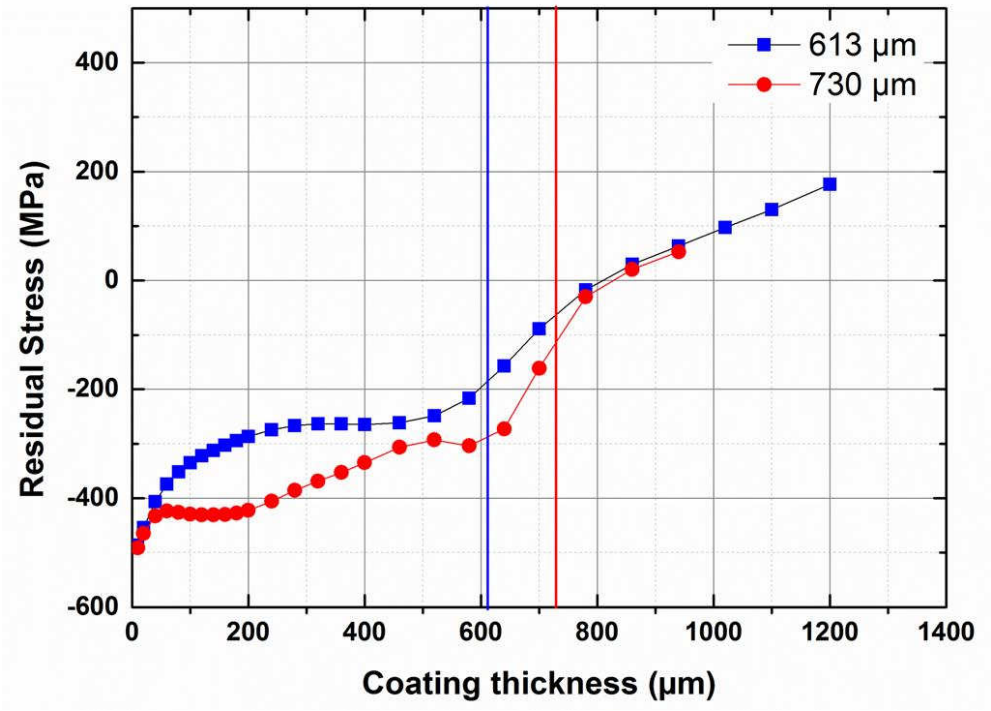

Figure 5: Residual stress distribution through coating/substrate system with the coating thickness of 613 µm and 730 µm, measured by the hole-drilling method. Blue line and red line represents the interface between coating and substrate with the coating thickness of 613 µm and 730 µm respectively.

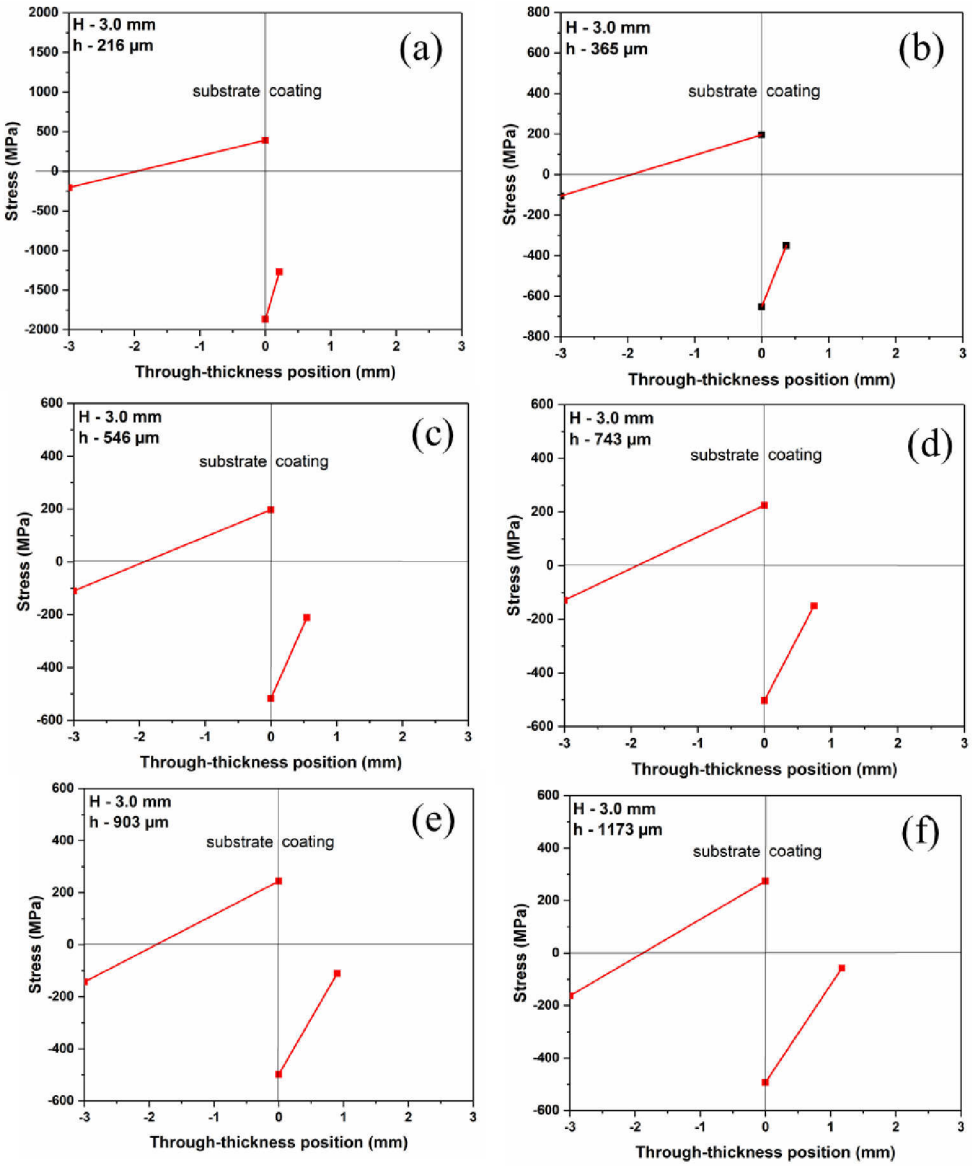

Figure 6: Estimated stress distribution through thickness of coating/substrate system with substrate thickness of H = 3.0 mm, coating thickness of h = (a) 216 µm (b) 365 µm (c) 546 µm (d) 743 µm (e) 903 µm, and (f) 1173 µm.

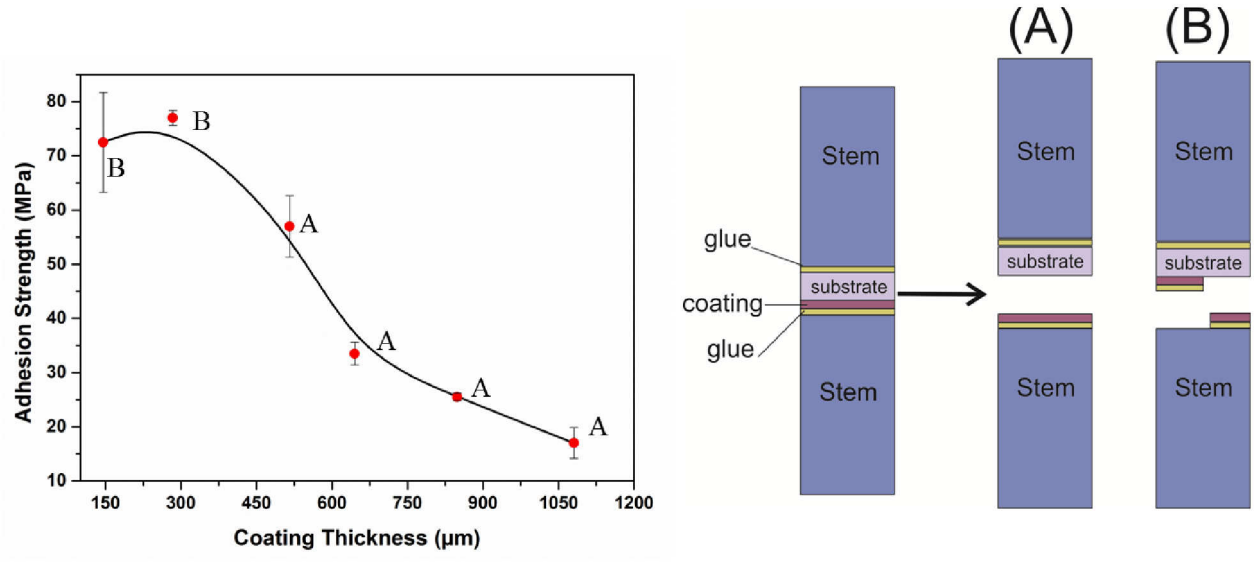

Figure 7: Adhesion-strength variation with coating thickness, where the black line is guideline to follow the data points. Failure mode corresponding to each data point is represented by A and B. (b) schematic of failure modes, failure mode A – adhesive failure i.e. the failure at the interface between coating and substrate; failure mode B – mixed mode i.e. failure partly at the interface between coating and substrate and partly between glue and coating.

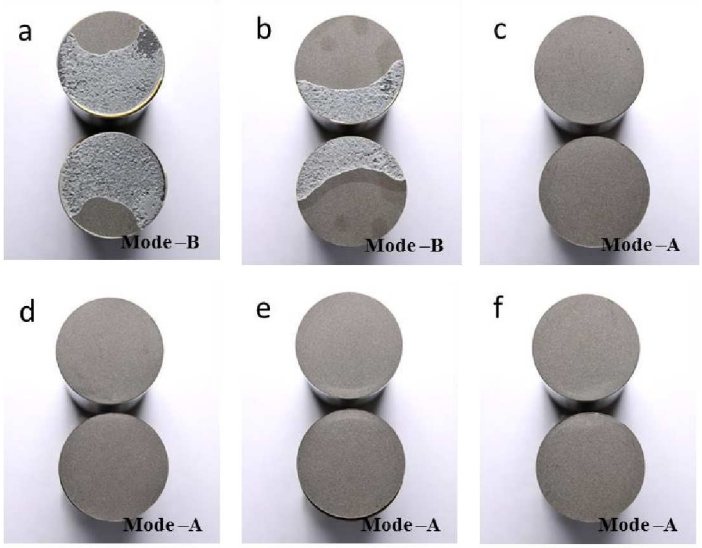

Figure 8: Photos of failures after bond-strength test of coating with coating thickness of, (a) 146 µm, (b) 284 µm, (c) 516 µm, (d) 645 µm, (e) 849 µm, and (f) 1081 µm

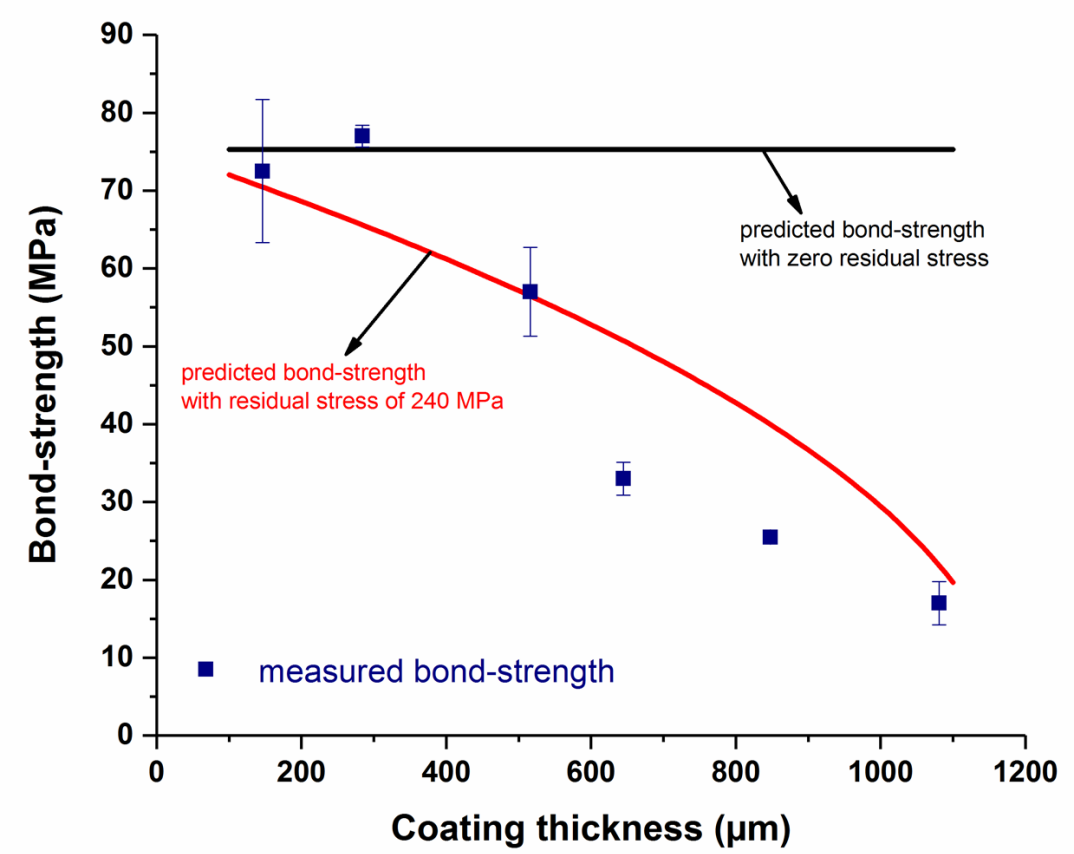

Figure 9. Comparison of predicted and experimentally measured bond-strength of cold sprayed IN 718 coating on IN 718 substrate.